Incorporating cost-efficient selection of feeders in a novel adaptive UFLS scheme for application in low-inertia renewable-intensive grids considering voltage stability analysis

Mehrdad Bagheri-Sanjareh [a,*], Martijn Janssen [b], Jorrit Bos [c], Aleksandar Boricic [c], Peter Palensky [a], Marjan Popov [a]

[a] Delft University of Technology, Faculty of EEMCS, Mekelweg 4, Delft, 2628CD, the Netherlands
[b] Alliander N.V., the Netherlands
[c] TenneT TSO BV, the Netherlands

ARTICLE INFO

Keywords:
Frequency control
Under-frequency load shedding (UFLS)
Inertia
RoCoF
Voltage stability
Power balance
Renewable resources proliferation

ABSTRACT

Conventional Under-Frequency Load Shedding (UFLS) schemes may lead to over-/under-shedding, and they are not quite reliable for application in low-inertia renewable-intensive grids. This paper proposes an adaptive UFLS scheme suitable for low- and varying-inertia grids. It calculates the frequency event size and executes shedding loads equal to it. The Center-of-Inertia (CoI) Rate of Change of Frequency (RoCoF) is used after estimating it using local frequency measurements. The fast voltage stability indices of loads are used to define their shedding share coefficients according to their level of weakness with respect to voltage stability. Moreover, the steady-state voltage analysis is conducted to determine the maximum limit of active/reactive power decrease at each load bus to limit the shedding amount which avoids violating permissible voltage limits. To maintain the practicality of this scheme, the selection of feeders for disconnection is considered for realizing the calculated shedding amount. To evaluate the proposed UFLS scheme, it is tested on IEEE-39 bus test network with different penetration levels of renewable resources. The realized shedding amount is slightly different from the calculated one considering that the exact amount of load cannot be shedded through feeders' disconnection. However, the frequency is stabilized in all case studies.

1. Introduction

The continuity of electric power supply based on power grid demands depends on its stability. One stability aspect is frequency stability which is guaranteed as long the equilibrium between electricity demand and supply is maintained [1,2]. Major frequency stability disturbances are loss of large generation units or loads outages, upsetting the demand-supply balance and causing frequency deviations that can lead to blackouts if not promptly mitigated [3–5].

As a last-resort emergency control scheme, Under-Frequency Load Shedding (UFLS) is widely employed to counteract severe frequency drops by intentionally disconnecting load. It plays a critical role in preserving frequency stability and preventing system collapse under extreme operating conditions [6].

Conventional UFLS strategies are based on and fixed load shedding steps and predefined frequency thresholds [7]. This makes them straightforward and also widely-used in most power grids [8]. However, their main drawback is that may result in either over-shedding or under-shedding of load which stems from their inadaptability to real-time system conditions. For instance, they do not account for variations in network topology, generation mix, or system inertia [7].

These UFLS schemes are not functioning quite reliably, in modern power systems, mostly due to the proliferation of Renewable Energy Sources (RESs). In contrast to conventional synchronous generators, RESs lack inherent inertia, causing higher frequency deviations with higher rates. Therefore, the increased growth of wind turbine generators and photovoltaic systems have caused the overall inertia to decrease and vary more compared to a conventional grid that is mostly supplied by synchronous generators. [9]. The blackouts of Spain in 2025, UK in 2019 and South Australia in 2016 are examples of frequency instability incidents, one contributory cause of which was the low inertia as the results of increased growth of RESs [10–13]. Therefore, the conventional

* Corresponding author.
E-mail address: M.Bagheri-sanjareh@tudelft.nl (M. Bagheri-Sanjareh).

UFLS schemes are no longer quite reliable in maintaining frequency stability of modern low-inertia grids, which highlights the need for more adaptive and reliable UFLS schemes [7].

The use of rate of change of frequency (RoCoF) can improve the performance of conventional UFLS schemes. On this basis, semi-adaptive schemes, that use both frequency and its rate, were developed with relatively faster detection of disturbances [7]. In [14], a multi-stage semi-adaptive UFLS scheme is proposed. In 1st stage, RoCoF is employed for load shedding while the frequency thresholds are used for the subsequent stages. Even though semi-adaptive schemes are more promising than conventional ones, they may still lead to under-/over-shedding. This is because they are indifferent towards grid operation conditions and dynamic parameters, which is in particular the overall inertia that can help estimate the frequency event size for load shedding accordingly.

Adaptive UFLS schemes are more advanced, being capable of dynamically determining both the location and the amount of load shedding. This is realized by leveraging wide-area monitoring measurement with high-resolution and in real time like those provided by PMUs [15,16].

In [17], an Adaptive UFLS (AUFLS) scheme is proposed that considers the primary responses of the generators as well as the virtual inertia. However, the authors have assumed the frequency deviation to be similar across the network which is incorrect. Another single-stage scheme is proposed in [18] based on the transient energy concept to calculate the required amount of shedding. The authors of [19] have used the frequency nadir prediction to propose a multi-stage AUFLS scheme. The number of shedding thresholds and the overall number of stages are modified to ensure only adequate number of loads are disconnected. The authors of [20] have proposed an AUFLS scheme that detect a Loss of Generation (LoG) by analyzing nodal current and voltage variations provided by PMUs. One important drawback of this scheme is that it can only consider one LoG event at a time. The other drawback that also exists in [18] and [19] is that they significantly rely on power system models and parameters which are quite inconstant due to high RESs penetration. In [21], the amount of load shedding at each stage is adaptively determined to decrease the overall demand shed for UFLS. Following the same strategy, the authors of [22] have proposed the adjustment of the amount of load shedding based on a frequency stability boundary curve that considers both the frequency deviations and RoCoF values. One important shortcoming of the mentioned studies [17–20] is that they have not considered the effect of load shedding on voltage stability and profile considering that disconnecting feeders also means decreasing reactive power in addition to active power.

To improve voltage stability, the authors of [23] have optimally determined the amount of load shedding for each bus considering the voltage drops. An AUFLS scheme is proposed in [24] which is a single-stage centralized one that employs the center of inertia (COI) RoCoF to estimate the required shedding amount. The authors have conducted reactive power-voltage sensitivity analysis which helps shedding more loads at weaker buses in term of voltage stability. In [25], a UFLS is proposed based on voltage stability and RoCoF of each zone. For this purpose, the weakest buses are ranked according to reactive power-voltage analysis. However, the authors have used a semi-adaptive UFLS scheme that is incapable of calculating the required amount of shedding and therefore over-/under-shedding cannot be avoided. The works in [15,26] ranks buses based on Fast Voltage Stability Index (FVSI), aggregating them for UFLS. One important drawback of [15,24–26] is that they have used static power flow-based studies for reactive power-voltage analysis. Consequently, they have not studied the after-event conditions to consider the effect of decreased reactive power on voltage profile due to load shedding. To take this into account, this paper proposes conducting dynamic simulations to measure the maximum active/reactive power decrease limit at each load bus without violating voltage limits. Moreover, these works including [23] have not attempted to minimize the cost of UFLS which is contrarily considered here. Also, the authors of [15,25] have assumed the shedding amount as a continuous variable which is incorrect as in reality the disconnection of feeders cannot result in any desired shedding amount.

In [26], a centralized UFLS scheme selects enough number of feeders in real-time to closely match the required shedding amount. On the contrary, the feeder selection method of this paper is decentralized and selects feeders before the event occurrence. The fact that it is not centralized makes it suitable for real-time application, not imposing any delays regarding shedding amount calculation, feeder selection and communication of signals and commands. The authors of [27] have proposed a conventional multi-stage UFLS scheme that uses a clustering method to group feeders such that their combined behavior is overall constant over time. The authors of [28] have presented a chance-constrained approach to select a subset of feeders that ensures that adequate loads are disconnected with high probability in spite of uncertainty of feeders' demands. It is worth noting that these probabilistic and clustering approaches cannot guarantee a good accuracy for shedding the required amount of load in real-time. To avoid this, in this paper, the demands of the selected feeders are updated every 30 min for different shedding amounts which takes into account the variation of feeders' demand.

The proposed AUFLS scheme uses the CoI-RoCoF-based method proposed in [7] to locally estimate CoI-RoCoF which is used to calculate and shed enough loads in two stages. Using the FVSI, the load buses are ranked from weak to strong and their shedding share coefficients are determined accordingly. The steady-state voltage analysis is conducted to determine the maximum limit of active/reactive power decrease at each load bus to limit shedding which results in not violating the allowable voltage limits. A portion of shedding share of some loads may not be realized and therefore, their shedding share coefficients will be modified such that other loads will provide the rest of their share. Each load bus will disconnect the number of feeders to satisfy the required shedding amount according to these coefficients. Since the exact required shedding amount can be executed by disconnecting feeders, discrete shedding steps are defined that different groups of feeders are aggregated for each discrete shedding step. The group of feeders of the corresponding shedding step that is the closest to the required shedding amount will be disconnected. Moreover, feeders of each load block are aggregated based on the lowest shedding cost as their shedding costs are not similar due to their different importance. The contributions of this works with respect to the previous works are: 1) Use of FVSI and steady voltage analysis to determine shedding share of load buses across the grid to avoid voltage instability issues while stabilizing the frequency, 2) Considering disconnection of feeders in the process of determining the required shedding amount to maintain practicality, 3) Operating in a decentralized manner using local estimation of CoI-RoCoF and lack of reliance on communication links and central control to calculate and execute the required shedding amount, 4) Considering feeders' disconnection for executing the required load shedding with the minimal shedding cost. These contributions with respect to the previous works are summarized in Table 1.

The rest of this paper are organized as follows: Section 2 describes the details of the proposed UFLS while section 3 conducts simulation studies and analysis to evaluate the performance of the UFLS scheme with respect to the methodologies of previous works. Section 4 concludes the paper results and analysis.

2. Proposed UFLS scheme

The proposed AUFLS scheme sheds enough loads at two stages to intercept the frequency decline when the frequency reaches the shedding thresholds of each stage. It consists of the following tasks: 1) Calculating the required shedding amount for each selected load bus using CoI-RoCoF and overall grid inertia, 2) CoI-RoCoF estimation methodology using local frequency measurement, 3) Calculating the maximum permissible decrease in active/reactive power demand of

Table 1
Comparison on the existing literature review of UFLS schemes.

Ref. No	Adaptive?	Voltage stability method	Feeder selection method	Decentralized?	Minimizing shedding cost?
[7]	Yes	Not considered	Not considered	Yes	No
[15]	Yes	Fast voltage stability index	Not considered	No	No
[17]	Yes	Not considered	Not considered	No	No
[18]	Yes	Not considered	Not considered	No	No
[19]	Yes	Not considered	Not considered	No	No
[20]	Yes	Not considered	Not considered	No	No
[21]	Yes	Not considered	Not considered	No	No
[22]	Yes	Not considered	Not considered	No	No
[23]	Yes	Considering voltage drops after event	Not considered	No	No
[24]	Yes	Reactive power-voltage sensitivity analysis	Not considered	No	No
[25]	Yes	Reactive power-voltage sensitivity analysis	Not considered	No	No
[26]	Yes	FVSI	Not considered	No	No
[27]	No	Not considered	Yes	No	No
[28]	Not considered	Not considered	Yes	Not considered	No
This paper	Yes	1) FVSI and 2) Steady-state voltage stability analysis	Yes	Yes	Yes

each load considering steady-state voltage profile analysis, 3) Calculating the shedding share of each load bus according to FVSI and their reactive power decrease limit, 4) aggregating the feeders of each load bus, minimizing the feeders' shedding cost and taking into account the maximum permissible decrease in reactive power demand of each load. Each of these tasks are explained in order in the following sections.

2.1. Calculation of the required shedding amount using CoI-RoCoF and overall grid inertia

The frequency decline occurs when the active power balance between demand and generation is disrupted and demand exceeds generation. To model the frequency dynamics of a power grid, the generator swing equation is studied:

$$P_i^m - P_i^e = \Delta P_i = 2H_i RoCoF_i(t=t_0^+) + D_i \Delta f_i(t=t_0^+) \tag{1}$$

where ΔP_i denotes the difference of P_i^m and P_i^e which are the mechanical and electrical generated power by a synchronous generator while $\Delta f_i(t=t_0^+)$, $RoCoF_i(t=t_0^+)$, H_i and D_i represent the after-event frequency deviation, RoCoF, damping and inertia time constant of the generator rotor in per unit, respectively. Considering that $\Delta f_i(t=t_0^+)$ is negligible, Eq. (1) can be modified for UFLS application [7] as:

$$P_i^m - P_i^e = \Delta P_i = 2H_i RoCoF_i(t=t_0^+) \tag{2}$$

Adapted from Eq. (2), Eq. (3) represents the center-of-inertia (CoI) swing equation which can calculate the overall active power imbalance in a grid with more than one synchronous generator:

$$\Delta P_{CoI} = 2H_{CoI} RoCoF_{CoI}(t=t_0^+) \tag{3}$$

where ΔP_{CoI}, $RoCoF_{CoI}(t=t_0^+)$ and H_{CoI} represent the same parameters in Eq. (2) that instead correspond to the grid CoI. Each can be calculated as presented in the following:

$$\Delta P_{COI} = \frac{\sum_{i=1}^N \Delta P_i S_i}{\sum_{i=1}^N S_i} \tag{4}$$

$$H_{COI} = \frac{\sum_{i=1}^N H_i S_i}{\sum_{i=1}^N S_i} \tag{5}$$

$$RoCoF_{CoI}(t=t_0^+) = \frac{\sum_{i=1}^N \left(H_i S_i RoCoF_i(t=t_0^+)\right)}{\sum_{i=1}^N (H_i S_i)} \tag{6}$$

The overall active power imbalance can be calculated in MW using Eq. (7) which is obtained by replacing the overall inertia term in Eq. (3) by Eq. (5):

$$\Delta P_{CoI}(p.u) \sum_{i=1}^N S_i = 2 \sum_{i=1}^N (H_i S_i) RoCoF_{CoI}(t=t_0^+) \tag{7}$$

where $\sum_{i=1}^N H_i S_i$ represents the overall kinetic energy of the grid. The left-hand side of Eq. (7) calculates ΔP_{CoI} in MW. Since the CoI inertia after inertia is not known, a relatively low value is chosen to calculate the required shedding amount for 1st stage as presented in Eq. (8):

$$P^{1st} = 2\left(\sum_{i=1}^N H_i S_i\right)_{low} RoCoF_{1st} \tag{8}$$

where $\left(\sum_{i=1}^N H_i S_i\right)_{low}$ is the selected value for the overall kinetic energy and $RoCoF_{1st}$ is the estimated 1st stage CoI-RoCoF while P^{1st} is the 1st stage shedding amount which is less than the actual event size since $\left(\sum_{i=1}^N H_i S_i\right)_{low}$ is less than the actual overall kinetic energy after the occurrence of the event. The CoI-RoCoF changes after 1st stage shedding can be used to calculate the after-event overall kinetic energy using Eq. (9):

$$\left(\sum_{i=1}^N H_i S_i\right)_{act} = \frac{P_{1st}}{2(RoCoF_{1st} - RoCoF_{2nd})} \tag{9}$$

where $RoCoF_{2nd}$ is the CoI-RoCoF after 1st stage shedding. Then, the 2nd stage shedding amount, which is equal to the difference of the event size and the 1st stage shedding amount, can be calculated using Eq. (10):

$$P^{2nd} = P_{Ev} - P^{1st} = \left(2\left(\sum_{i=1}^N H_i S_i\right)_{act} RoCoF_{1st}\right) - P^{1st} \tag{10}$$

where P_{Ev} represents the event size. Using Eq. (9), Eq. (10) can be rewritten as follows:

$$P^{2nd} = \left(\frac{RoCoF_{1st}}{(RoCoF_{1st} - RoCoF_{2nd})} P_{1st}\right) - P^{1st} \tag{11}$$

Eq. (11) shows that the change in CoI-RoCoF after 1st stage shedding can be used to calculate the actual event size. Since the CoI-RoCoF is locally estimated, load bus i will disconnect its share of the required shedding amount if the local frequency drops below its corresponding thresholds as presented in Eq. (12). For instance, if the frequency does not reach the 2nd stage shedding threshold after executing the 1st stage, 2nd stage will not be executed, meaning that 1st stage shedding was sufficient to stop the frequency decline.

$$\begin{cases} P_i^{1st} = P^{1st} K_i & if: f < f_{1st}^{tresh} \\ P_i^{2nd} = P^{2nd} K_i & if: f < f_{2nd}^{tresh} \end{cases} \tag{12}$$

where K_i is the shedding share coefficient of i^{th} load bus while f_{1st}^{tresh} and f_{2nd}^{tresh} are the frequency shedding thresholds of 1st and 2nd stages, respectively.

As far as the shedding strategy is concerned, the 1st stage provides an early response and slows down the frequency decline if not stop it, while the 2nd stage of shedding is initiated if the first stage is insufficient. The observation of the change in the CoI-RoCoF after 1st stage helps calculating the overall event size as presented in Eq. (10). The shedding amount of 2nd stage is equal to the event size minus the shedding amount of 1st stage. Therefore, the overall shedding amounts of both stages would be equal to the event size and overshedding is prevented.

2.2. CoI-RoCoF estimation methodology

The proposed AUFLS scheme uses the CoI-RoCoF to determine the required shedding amount to stabilize the frequency decline. Fig. 1(a) shows the overall procedure for processing the frequency measurement to obtain the CoI-frequency and RoCoF. Also, Fig. 1(b) demonstrates the use of zero-crossings in the waveform of the frequency second derivative to detect the inflection points which are critical for obtaining the CoI frequency and RoCoF. The frequency of the low-pass filter is 100 Hz to suppress measurement noises [7]. It is worth noting that using this approach, the local frequency can be used to estimate the CoI-RoCoF without needing to transfer all bus frequency data to a control center to calculate the CoI frequency and the CoI-RoCoF. Therefore, communication links are not required since the shedding decisions are taken locally including the amount of shedding at each selected bus. Regarding the locations of measurements, each selected bus for load shedding requires the local frequency measurement for CoI-RoCoF estimation. The local frequency measurement and independence on communication links help realizing a decentralized AUFLS scheme. The delay of measurements are assumed to be negligible while the delay of 0.2 seconds is considered for the overall function of relays and feeder breakers.

2.3. Calculating the maximum allowable decrease of reactive power of loads

The shedding of loads also affects the voltage profile since reactive power demands are also shed. While the aim is stabilizing the frequency, the steady-state voltage of buses should also remain within acceptable limits (0.95 p.u. – 1.05 p.u). For this purpose, the maximum permissible decrease in reactive power of loads allocated for shedding is essential to be considered.

Moreover, the outage of each generator is considered as a frequency event that may be severe enough to require UFLS. After the occurrence of each generator outage, both active and reactive power of loads, which are allocated for UFLS, are proportionately decreased in fixed steps. As long as the voltage limits of the bus are not violated, the active and reactive power of its corresponding load keeps decreasing unless it has reached its demand size. Flowchart in Fig. 1(c) summarizes this process. Of all the maximum permissible values per all generator outage events, the minimum value is chosen for each load since it is not known which event will take place.

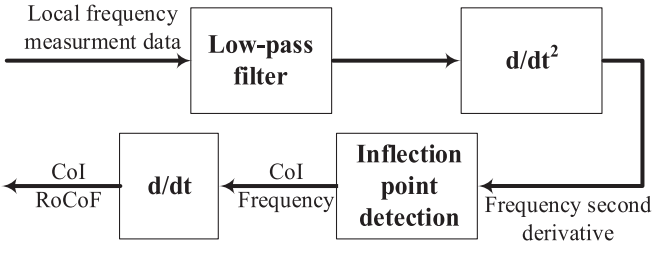

Fig. 1(a). Overall process of CoI-RoCoF estimation using local frequency measurement.

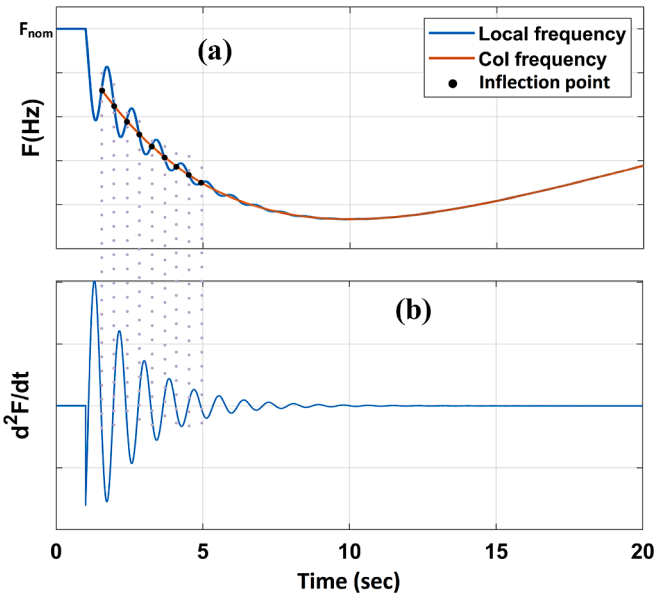

Fig. 1(b). Inflection point detection for CoI-RoCoF estimation.

2.4. FVSI-based sharing of required load shedding

The FVSI which is explained in [15] can rank load buses from weak to strong in terms of voltage stability. In this regard, those buses with the higher FVSI are closer to voltage collapse and therefore, they have more priority for UFLS since shedding reactive power will improve their voltage stability. The following equation will be used to determine shedding share of each bus according to their FVSIs:

$$K_i = \frac{FVSI_i}{\sum_{i=1}^{N} FVSI_i} \tag{13}$$

where K_i and $FVSI_i$ denote the shedding share and FVSI of i^{th} load bus. The shedding share of each load must be enough such that the outage of the generator with the highest power generation can be controlled by the AUFLS. In case each load cannot satisfy its share either by its demand limit or voltage limits, the shedding share coefficients of loads will be redefined as follows:

$$K_i^{new} = \begin{cases} \dfrac{P_i^{Limit}}{P_G^{\max}} & i \in \ell \\ k_i + \left(\sum_{j \in \ell} \left(P_G^{\max} K_j - P_j^{Limit} \right) \right) \dfrac{k_i}{\sum_i k_i} & i \in \gamma \end{cases} \tag{14}$$

where ℓ represent the set of loads that can reach their shedding limit while γ represent the rest of the loads.

2.5. aggregating the feeders for UFLS at each load bus

While loads are represented individually by feeders at distribution level, at transmission level they are aggregated into single large loads, each representing the sum of multiple feeders as shown in Fig. 2(a). Frequency dynamics simulation studies are conducted on the transmission grid to determine the amount of load shedding at each load bus in case a frequency event occurs. However, in reality, feeders must be disconnected which may not realize the exact amount of load shedding. Despite this, shedding an amount close to the determined amount is possible. It is worth noting that feeders supplying power to the grid will not be considered for shedding, like those feeders with distributed resource generation that exceed their demand.

Eq. (15), which is developed based on the approach demonstrated in

```
1: Start
2: Initialize inputs (Generators set (G), UFLS loads set (L), Decrease increment (ΔP), voltage limits: Vmin & Vmax)
3: For each generator g ∈ G:
    a: Create outage event
    b: Initialize active load set (L → A)
    c: While A ≠ {}:
        i: Initialize RMS simulation
        ii: Run RMS simulation
            1: For each load i ∈ A:
                a: If (Pi ≠ 0) AND (Vmin < V < Vmax):
                    i: Decrease active power Pi = Pi − ΔP
                    ii: Decrease reactive power proportionally to active power and P.F.
                b: Else:
                    i: Record maximum permissible decrease in active/reactive power of load i for g
                    ii: Remove load i from A
    e: Restore all loads (L ← A)
4: Record maximum permissible decrease in active/reactive power of of each load per G
5: End
```

Fig. 1(c). Pseudo-code describing the overall process of determining the maximum permissible decrease in active/reactive power of loads allocated for UFLS.

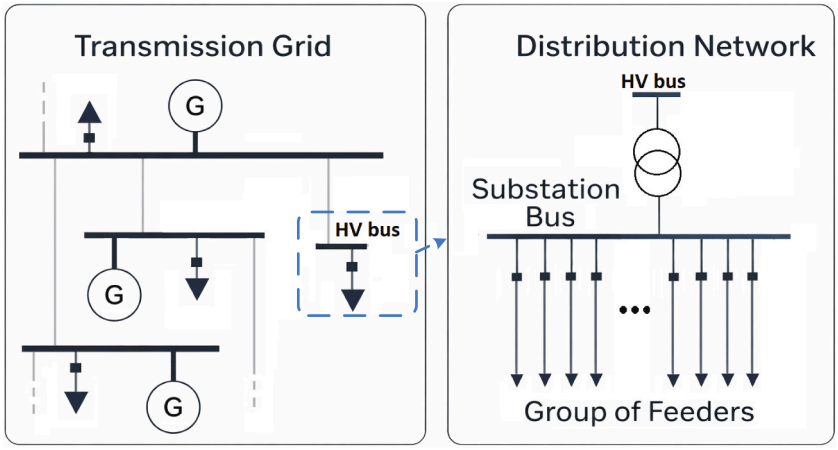

Fig. 2(a). Load presentation at transmission and distribution levels.

Fig. 2(b), can be used to convert the continuous shedding amount curve into discretized shedding levels. By aggregating feeders, each of these shedding levels can be almost achieved. For each 1st-stage shedding amount, those feeders that are not aggregated for shedding, will be aggregated similarly but for realizing each discrete shedding amount of 2nd stage.

$$TP = \Delta P.round(\frac{P^{1st}/P^{2nd}}{\Delta P}) \tag{15}$$

where TP and ΔP represent the achievable shedding amount and the discretization step, respectively.

The shedding cost of each feeder is different depending on their importance. Therefore, the feeders must be aggregated based on minimizing the overall shedding cost. At each bus, the feeder selection problem is formulated as a binary integer optimization problem that minimizes the total cost of selected feeders while satisfying a target power demand within a predefined tolerance. The decision variable x_i is binary for feeder i, such that:

$$x_i = \begin{cases} 1, & if selected \\ 0, & otherwise \end{cases} \tag{16}$$

The input parameters are M (total number of feeders at the bus), P_i (active power of feeder i (MW)), c_i (cost associated with feeder i), (TP^{1st} (1st stage target demand shedding (MW)), E (allowable tolerance (MW)) and Q_i^{max}(maximum allowable reactive power at bus i). The optimization problem of 1st stage aggregation of feeders can be defined as follows:

$$\begin{aligned} \min_{x_i} \quad & \sum_{i=1}^{M} c_i x_i \\ s.t. \quad & TP^{1st} \leqslant \sum_{i=1}^{M} p_i x_i \leqslant TP^{1st} + E \\ & \sum_{i=1}^{M} p_i x_i \leqslant P^{max} \\ & P^{max} = Q^{max}\left(\frac{P.F.}{\sqrt{1-P.F.^2}}\right) \\ & x_i \in \{0,1\}, \forall i = 1, \ldots, M \end{aligned} \tag{17}$$

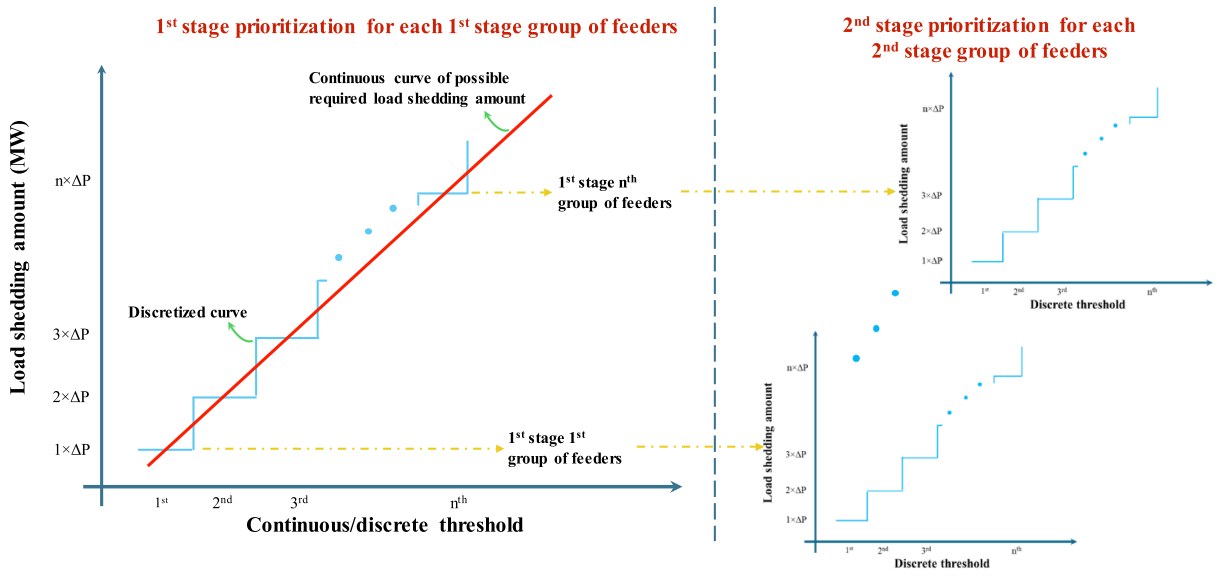

Fig. 2(b). Converting the continuous shedding amount into achievable shedding levels.

The 2nd stage optimization, parameters and variables are almost similar to that of 1st stage problem except that the decision variable y_j is binary for feeder *j*. such that:

$$y_j = \begin{cases} 1, & if selected \\ 0, & otherwise \end{cases} \tag{18}$$

Also, TP^{2nd} is the 2nd stage target demand shedding (MW). Therefore, the optimization problem of 2nd stage aggregation of feeders can be defined as follows:

$$\begin{aligned} &\min_{y_i} \quad \sum_{j=1}^{R} c_j y_j \\ &s.t. \quad TP^{2nd} \leqslant \sum_{j=1}^{R} p_j y_j \leqslant TP^{2nd} + E \\ &\sum_{j=1}^{R} p_j y_j \leqslant P^{\max} - \sum_{i=1}^{M} p_i x_i \\ &P^{\max} = Q^{\max}\left(\frac{P.F.}{\sqrt{1-P.F.^2}}\right) \\ &y_j \in \{0,1\}, \forall j \in R, R = \{i | x_i = 0\} \end{aligned} \tag{19}$$

In this paper, the genetic algorithm and MATLAB software program is used to solve these optimization problems. The decision variables for feeder-selection are binary. To provide adequate search diversity and evolutionary exploration, a population size of 100 and a maximum of 200 generations is adopted. A crossover fraction of 0.8 was used to promote recombination of promising solutions while an elite count of 5 was employed to ensure high-quality solutions. The optimizations were terminated when the function tolerance of 10^{-6} was satisfied or after 50 consecutive generations without significant improvement.

2.6. Overall AUFLS process

During the continuous grid operation, the values of the grid operation variables are gathered every 30 minutes including the active/reactive power generated and consumed by resources and loads, respectively. These are used to: 1) Determine FVSIs of each load bus, 2) update the initial conditions of the grid simulation studies which are used to determine the maximum decrease limit of each load's reactive power, 3) determine the shedding share coefficients of each load, 4) Aggregate groups of the feeders of each load bus to realize each shedding steps if required. In case of frequency event occurrence, the CoI-RoCoF will be estimated for both stages which will be used to calculate the required amount of shedding. Then, it is executed by disconnecting the aggregated feeders as discussed in the previous section. Fig. 3 demonstrates the overall process of the proposed AUFLS scheme in real time.

It is worth noting that the 30-min period is sufficient to calculate the reactive power limits and also to update the aggregated feeders accordingly. In case, these tasks are not realized in time because of early occurrence of the event in each period, the reactive power limits and the aggregated feeders from the previous period are still valid to be used. Moreover, the variations of the feeders' demands are assumed to be negligible during each 30-min periods.

3. Simulation studies

To evaluate the proposed AUFLS scheme, several simulation scenarios on the IEEE-39 bus network are studied with different penetration levels of RESs and different frequency events. The test network is demonstrated in Fig. 4. All synchronous generators are equipped with governors. The following buses are allocated for load shedding which cover different regions of the grid: Bus 04, Bus 08, Bus 16, Bus 20, Bus 23, Bus 25, Bus 29. These buses are equipped with PMUs which provide fast frequency measurement data which are used continuously for the proposed AUFLS scheme. The frequency thresholds of 1st and 2nd stages are 49.5 Hz [7] and 49.2 Hz, respectively. Choosing 49.2 Hz for 2nd stage shedding threshold would provide enough to estimate CoI-RoCoF again to calculate the event size and the shedding amount of 2nd stage. Following the similar pattern in [29], the allocated loads for AUFLS are represented by the feeders with power demand varying from 2.4 MW and 8 MW. For instance, loads bus 'Bus 04' with overall 500 MW/184 MVAr active/reactive power demand has 88 feeders. For each case study, the power demand of each feeder is randomly generated. Moreover, the base shedding cost (€/kWh) of each feeder is randomly generated once considering the different importance of each feeder; however, they remain constant. The specifications of each case study including their frequency events are presented in Table 2.

3.1. Case study 1

Table A1 in Appendix A presents reactive/active decrease limits of loads, allocated for AUFLS, along with their FVSI indices. The former, which can be achieved by steady-state voltage analysis, is demonstrated in Figs. 5(a–d) for some of the buses as the representative of all buses. It

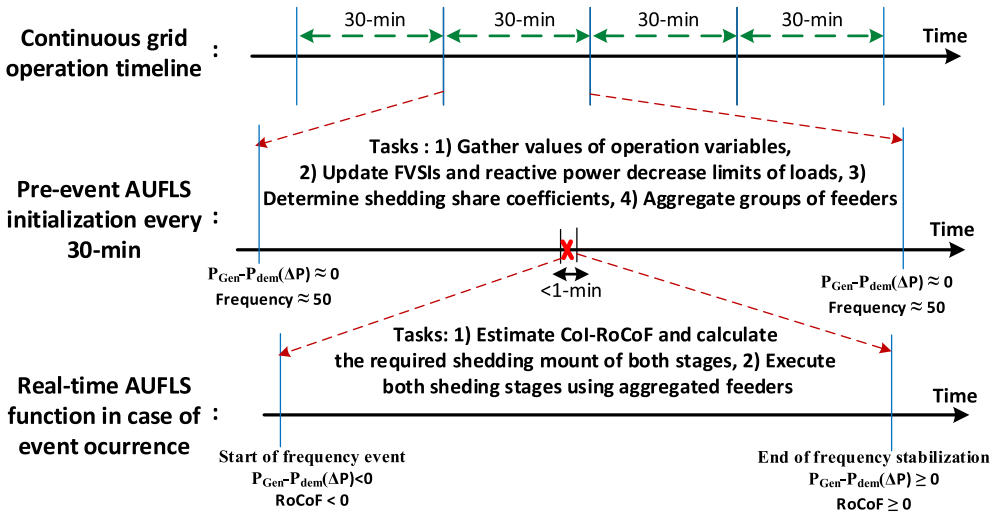

Fig. 3. Overall AUFLS process in real time.

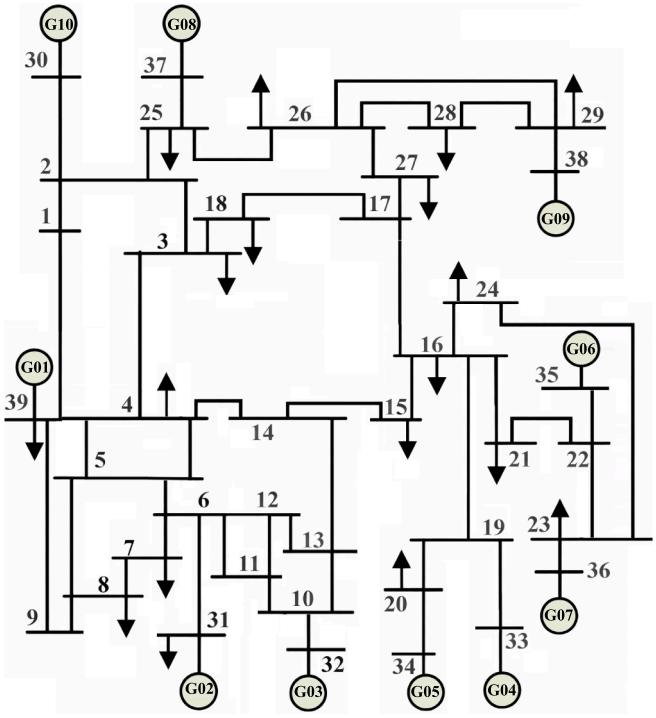

Fig. 4. IEEE 39 bus – test grid under study.

Table 2
Specifications of case studies.

Case study No.	Frequency event	$(\sum_{i=1}^{N} H_i S_i)_{act}$(MWs)
1	Outage of generator 'G5' while generating 508 MW	75670
2	Outage of generator 'G4' while generating 560 MW + Replacement of 'G7', 'G8' and 'G9' with IBRESs	66890
3	Outage of generator 'G8' while generating 550 MW + Replacement of 'G3', 'G5', 'G7', 'G9' and 'G10' with IBRESs + Reduction of power rating of generator 'G01' to 5 GW from 10 GW	34370

is evident that none of the loads are limited for reactive/active power decrease at these buses, which means AUFLS can be executed without causing steady-state overvoltage. Using the FVSI analysis, shedding share coefficients are also calculated as shown in Table A1.

The frequency event occurs at the 1st second. Using the value of 35000 MWs for $(\sum_{i=1}^{N} H_i S_i)_{low}$ and the CoI-RoCoF values obtained by the inflection points, the 1st stage shedding is calculated and executed. This is shown in Fig. 5 (e) which demonstrates the frequency variation and the AUFLS performance at 'Bus 04' as the representative of all load buses allocated for AUFLS. Table A2 in Appendix A summarizes the rest of frequency and relative numerical results including how the optimally aggregated feeders are shed to approximately realize the required shedding amount. Figs. 5 (f-k) compares the AUFLS performance by shedding the exact amount, that can be calculated by equations (8) and (10), and by shedding the amount that is achievable by disconnection of the feeders. As the required shedding amount with and without consideration of feeders' disconnection are close in value, the frequency curves of both cases are quite similar. The overall shedding amount in both cases is significantly less than the event size which is due to governors' response that slowed the frequency decline and prevented the 2nd stage shedding.

3.2. Case study 2

The results of steady-state voltage analysis in Table A3 in Appendix A show that even though the reactive/active decrease of some loads are limited, all are still sufficient to fulfill their shedding share defined by their corresponding FVSIs. For instance, the load of 'Bus 25' is determined to be 160 MW as also shown in Fig. 6(a). Despite this, its shedding coefficient is quite low such that this load can shed its small shedding share without violating the steady-state voltage limits of its bus.

The relatively low value of 35000 MWs is selected for the overall inertia. Using it and the CoI-RoCoF obtained by the inflection points to calculate and execute the 1st stage shedding. This is shown in Fig. 6(b and c) which demonstrate the frequency variation and the AUFLS performance at 'Bus 16' as the representative of all load buses allocated for the AUFLS. More numerical results are provided in Table A4 in Appendix A including the required shedding amounts of two stages with and without consideration of feeders' disconnection. It can be seen that the shedding amounts of each stage and also in total are relatively close with and without consideration of feeders' disconnection. Considering the feeders' disconnection, the frequency decline is still controlled with slight rise of frequency above the nominal value while the shedding amount is more realistic as feeders are considered. This is shown in Fig. 6

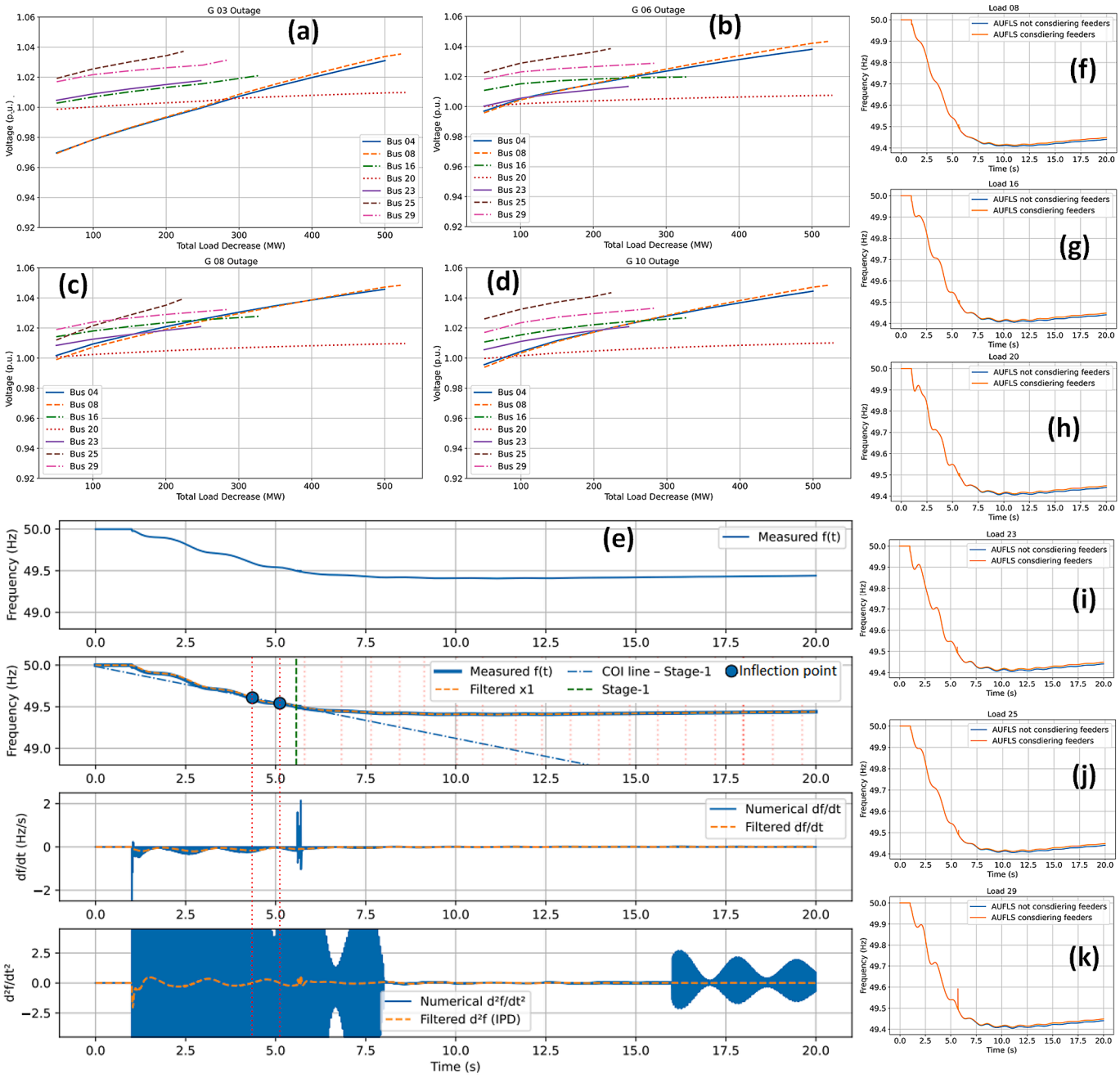

Fig. 5. Pre-event steady state voltage analysis, outage of generators (a) G 03, (b) G 06, (c) G08, (d) G 10, (e) Frequency variation and the overall AUFLS process, (f) Bus '08' frequency, (f) Bus '16' frequency, (f) Bus '20' frequency, (f) Bus '23' frequency, (f) Bus '25' frequency, (f) Bus '29' frequency.

(d and g) which compares the AUFLS performance by shedding the precisely calculated amount and the amount that is achievable by feeders' disconnection. Fig. 6(d-g) show that decreasing the discretization step to like 2.5 MW can improve the shedding accuracy as 207.77 MW and 375.68 MW are shedded in 1st and 2nd stages. This shows that the difference between the calculated amount and the achievable shedding amount is decreased compared to when the shedding discretization step is 5 MW.

3.3. Case study 3

Table A5 in Appendix A and Fig. 7(a) show that except 'Load 29', other loads can decrease their active/reactive power adequately to fulfill their shedding share defined by their corresponding FVSI indices. In this regard, Load 29' can decrease only 125 MW of its active and also its reactive power proportionately. Considering the outage of the 750 MW, which is the highest power generation of a single unit (G1'), the shedding share coefficient of this load becomes 0.166667 as mentioned in Table A5. The rest of the share of 'Load 29' is given to other loads according to section 3.4. By doing this, the maximum possible power reduction capability is allocated for UFLS at the selected buses considering their FVSIs and reactive power decrease limits.

The value of $(\sum_{i=1}^{N} H_i S_i)_{low}$ is selected to be 18750 MWs. It is used along with the CoI-RoCoF obtained by the inflection points to calculate and execute the 1st stage shedding. Fig. 7(b and c) demonstrate that the frequency of 'Bus 25' is restored after two stages of load shedding which shows successful performance of the proposed AUFLS scheme. Table A6 summarizes the rest of numerical results including how the optimally aggregated feeders are shed to realize the required shedding amounts of two stages with a good accuracy. The overall shedding amounts are

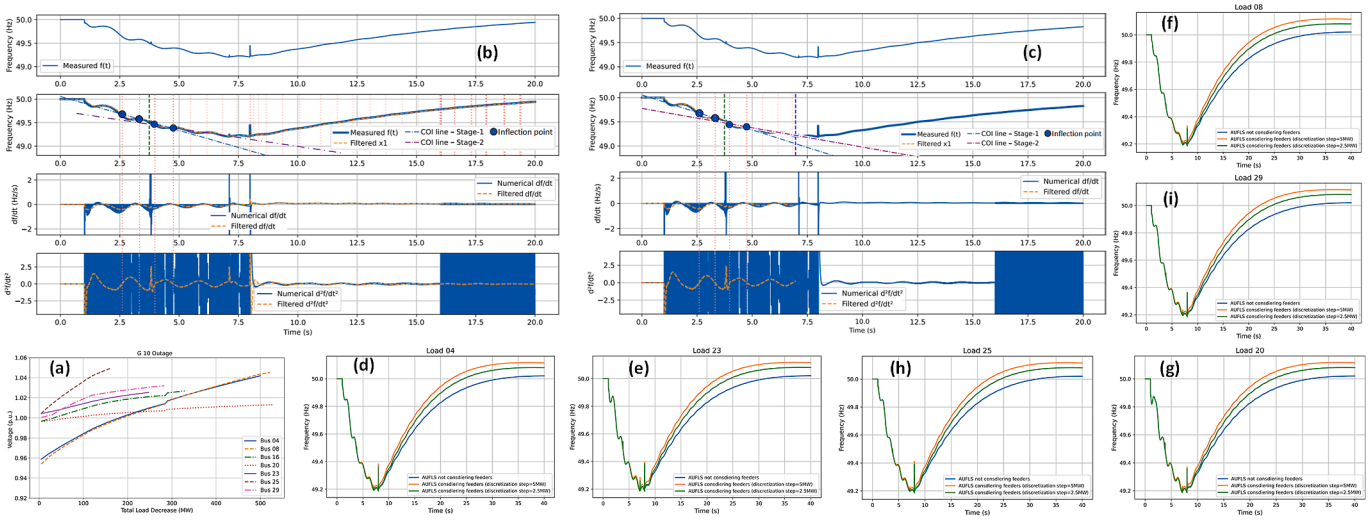

Fig. 6. (a)Pre-event steady state voltage analysis, outage of generator 'G 10', (b) Frequency variation and the overall AUFLS process considering feeders, (c) Frequency variation and the overall AUFLS process not considering feeders, (d-g) Frequency of load buses considering/not considering feeders disconnection.

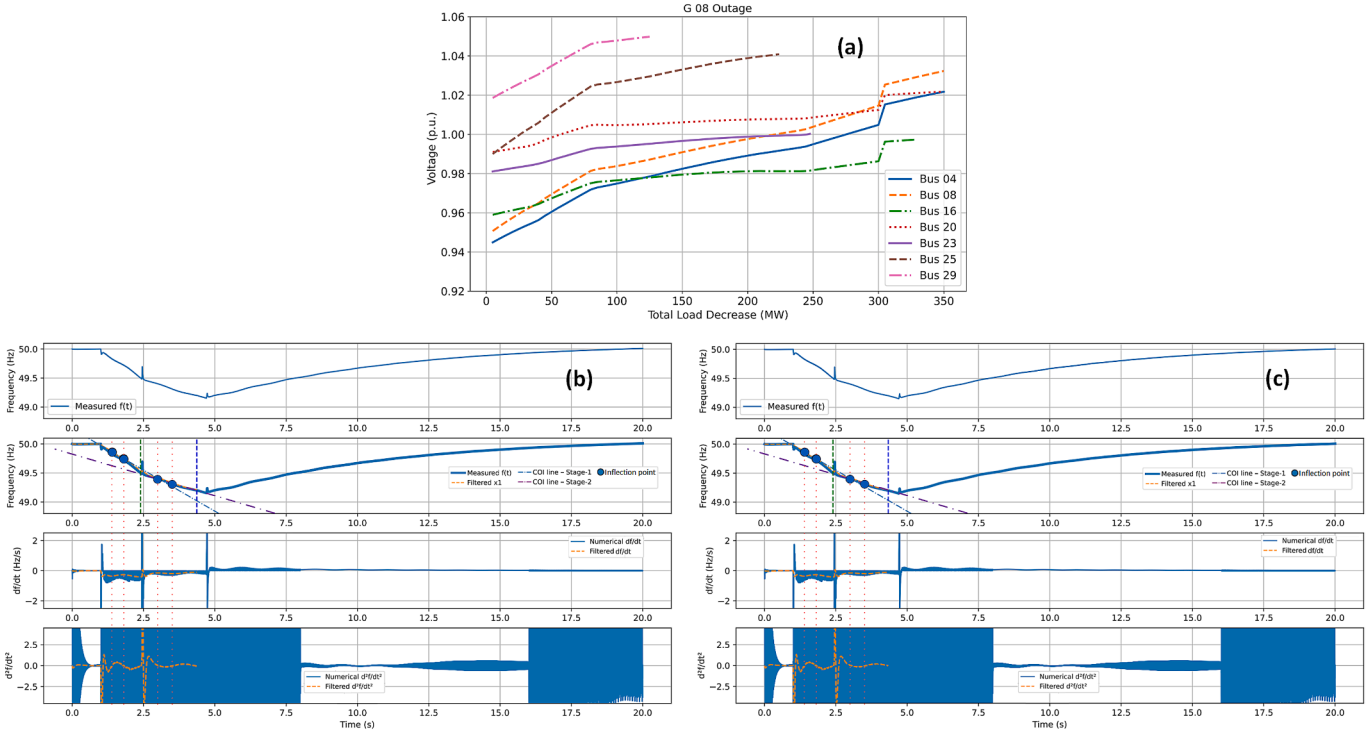

Fig. 7. (a) Pre-event steady state voltage analysis, outage of generator 'G 08', (b) Frequency variation and the overall AUFLS process considering feeders, (c) Frequency variation and the overall AUFLS process not considering feeders.

quite close to the event size with and without consideration of feeder' disconnection.

4. Discussion

The proposed UFLS works in a decentralized and therefore, it was not compared with the existing adaptive UFLS schemes that are mostly centralized which makes their control and decision-making mechanisms differ substantially. Moreover, the proposed decentralized UFLS scheme considers steady-state voltage conditions, FVSI and feeder selection which are neglected in previous works. Nonetheless, the proposed UFLS scheme can be assessed meaningfully against conventional fixed-threshold UFLS schemes that still remain widely employed in many power systems. The 1st shedding threshold for conventional schemes is commonly 49 Hz [30] and fixed percentage/amount of loads are shed, without actually considering the severity of the disturbance. However, the proposed UFLS scheme proactively determines the required shedding amount, being more aware of the grid conditions which always results in stabilizing the frequency above 49.2 Hz. This shows a relatively much better performance regarding the frequency nadir. Therefore, although a direct comparison with different UFLS schemes was not considered, the results demonstrate the effectiveness of the proposed approach and its improved frequency containment capability relative to conventional UFLS. The independency on communication links and central control along with feeder selection consideration make the proposed UFLS scheme applicable and practical unlike many previous

UFLS schemes.

5. Conclusion

A novel AUFLS scheme was proposed to stabilize the frequency in two shedding stages. Simulation results showed that the proposed AUFLS scheme managed to calculate and shed enough load to stop the frequency decline. In case one-stage shedding is not sufficient, the change in the CoI-RoCoF was used to calculate the amount of load almost equal to the event size, the shedding of which resulted in not just frequency stabilization but also restoration. The shedding share coefficient of each load bus was defined by FVSIs. This facilitated aggregating loads to shed more where grid is weaker in terms of voltage stability which is largely affected by the shortage of reactive power and low voltage profile. Moreover, the pre-event steady-state voltage analysis successfully calculated the maximum reactive power decrease limit of each load bus to avoid violating the permissible steady-state voltage limits after load shedding. The shedding share coefficients of loads were modified if their shedding share cannot be satisfied due to their maximum reactive power decrease limit.

Furthermore, feeders' disconnection for executing the load shedding was considered to investigate how accurately the calculated shedding amount of load can be realized. In this regard, the possible shedding amount was discretized into shedding steps and to realize each shedding step, a unique combination of feeders was considered. As the demand of feeders change over time and their shedding cost is different from one another, the combinations of feeders were scheduled for each shedding step on a periodic. The shedding step that is closest to the exact shedding amount is executed by disconnecting its allocated feeders. Through this approach, the frequency is still stabilized; however, the shedding amount and the settled frequency were insignificantly different. By decreasing the discrete shedding steps, the difference between the calculated and the achievable shedding amounts can be decreased.

CRediT authorship contribution statement

Mehrdad Bagheri-Sanjareh: Writing – review & editing, Writing – original draft, Visualization, Validation, Software, Resources, Methodology, Investigation, Formal analysis, Data curation, Conceptualization. **Martijn Janssen:** Resources, Funding acquisition. **Jorrit Bos:** Supervision. **Aleksandar Boricic:** Supervision. **Peter Palensky:** Supervision. **Marjan Popov:** Writing – review & editing, Supervision, Software, Resources, Project administration, Methodology, Funding acquisition, Validation.

Declaration of competing interest

The authors declare that they have no known competing financial interests or personal relationships that could have appeared to influence the work reported in this paper.

Acknowledgement

This research work is financially supported by Alliander N.V., which is gratefully acknowledged.

Appendix A

Table A1
Data for initializing AUFLS (Case study #1).

Bus No.	Active/reactive power limit (MW/MVAr)	FVSI index	Shedding share coefficient
04	500/184	0.035461	0.07076
08	500/169.23	0.039188	0.07820
16	329/32.3	0.124104	0.24763
20	528/88	0.056777	0.11329
23	247/84.6	0.057307	0.11435
25	224/47.2	0.034555	0.06895
29	283.5/26.9	0.153774	0.30683

Table A2
Simulation results of frequency controlling using AUFLS (Case study #1).

Bus No.	1st stage CoI-RoCoF (Hz/s)	1st stage shedding amount (MW)	1st stage shedded amount by feeders (MW)	Aggregated feeders' No./Power/cost (€)	Overall feeders shedding cost (€)
04	−0.0947	8.575	10.1	{(53/ 4.11/48.75), (56/2.44/24.9), (80/3.45/35.07)}	108.73
08	−0.0947	9.760	10.03	{(5/2.82/30.41), (54/4.29/44.91), (129/2.92/30.43)}	105.75
16	−0.0973	29.385	30.09	{(13/3.0/34.8), (16/2.88/43.48), (19/2.73/34.64), (37/3.848/50.62), (41/2.98/33.45), (48/2.71/35.97), (49/2.566/30.5), (56/3.317/40.6), (63/3.38/44.76), (81/2.678/27.77)}	376.58
20	−0.0830	12.319	15.06	{(49/2.52/26.1), (124/3.30/34.91), (129/2.45/29.66), (141/3.97/41.23), (169/2.815/29.34)}	161.24
23	−0.0979	14.584	15.24	{(2/2.42/45.14), (11/3.84/52.0), (16/2.89/43.341), (50/6.09/86.68)}	227.17
25	−0.0897	8.271	10.15	{(31,5.36/58.04), (46/4.79/64.36)}	122.40
29	−0.0929	39.624	40.04	{(4/3.49/38.59), (13/4.63/86.42), (14/4.59/54.79), (17/4.09/55), (21/2.45/48.96), (22/2.68/48.46), (44/2.67/37.43), (51/4.23/56.97), (52/4.54/91.45), (74/3.33/58.9), (75/3.34/36.16)}	613.14
Total	–	122.518	130	–	1715.01

Table A3
Data for initializing AUFLS (Case study #2).

Bus No.	Active/reactive power limit (MW/MVAr)	FVSI index	Shedding coefficient
04	485/ 178.48	0.038244	0.086605
08	515/173.64	0.040198	0.091030
16	329/32.3	0.119722	0.271117
20	528/88	0.056159	0.127176
23	247/84.6	0.037771	0.085534
25	160/33.57	0.006187	0.014011
29	283.5/26.9	0.143307	0.324528

Table A4
Simulation results of frequency controlling using AUFLS (Case study #2).

Bus No.	1st stage CoI-RoCoF (Hz/s)	1st stage shedding amount (MW)	1st stage shedding amount (MW) by feeders	2nd stage CoI-RoCoF (Hz/s)	2nd stage shedding amount (MW)	2nd stage CoI-RoCoF (Hz/s) by feeders	2nd stage shedding amount (MW) by feeders
04	−0.15058	17.80	20.03	−0.09665	29.4	−0.09467	35.06
08	−0.15020	19.14	20.04	−0.09747	32.94	−0.09472	35.09
16	−0.14458	54.78	55.01	−0.09956	109.4	−0.09730	115.04
20	−0.13291	23.66	25.07	−0.08466	38.98	−0.08308	45.07
23	−0.14919	17.86	20.10	−0.10002	32.81	−0.09793	40.06
25	−0.16377	3.21	5.12	−0.09215	3.92	−0.08971	10.04
29	−0.16252	73.84	75.04	−.09527	96.59	−0.09287	100.02
Total	–	210.31	220.41	–	344.04	–	380.38

Table A5
Data for initializing UFLS (Case study #3).

Bus No.	Active/reactive power limit (MW/MVAr)	FVSI index	Shedding coefficient
04	330/121.44	0.084407	0.177201
08	305/102.83	0.142042	0.298197
16	329/32.3	0.050542	0.106106
20	245/54.83	0.011296	0.023715
23	245/83.74	0.041813	0.087780
25	224/47.2	0.066845	0.140333
29	125/11.86	0.090700	0.166667

Table A6
Simulation results of frequency controlling using AUFLS (Case study #3).

Bus No.	1st stage CoI-RoCoF (Hz/s)	1st stage shedding amount (MW)	1st stage shedding amount (MW) by feeders	2nd stage CoI-RoCoF (Hz/s)	2nd stage shedding amount (MW)	2nd stage CoI-RoCoF (Hz/s) by feeders	2nd stage shedding amount (MW) by feeders
04	−0.29183	38.78	40.03	−0.17578	58.75	−0.17322	57.54
08	−0.29744	66.52	67.50	−0.17543	95.64	−0.17250	92.51
16	−0.26868	21.38	22.52	−0.17691	41.21	−0.17532	42.57
20	−0.24843	4.42	5.04	−0.17918	11.43	−0.15932	12.59
23	−0.25345	16.68	17.57	−0.17833	39.61	−0.17722	40.03
25	−0.28319	29.80	30.02	−0.17363	47.23	−0.17179	47.56
29	−0.26688	33.36	32.56	−0.17619	64.81	−0.17446	62.53
Total	–	210.96	215.24	–	358.68	-	355.33

Data availability

All data are avaiable in the paper or relevant data are referenced.

References

[1] Bagheri-Sanjareh M, Popov M. BESS and PV systems application for optimal microgrid operation with frequency security constraints. Sustain Energy Grids Networks 2025:102103.

[2] Ullmark J, Göransson L, Johnsson F. Frequency reserves and inertia in the transition to future electricity systems. Energy Syst 2024;15(4):1527–60.

[3] Ulbig A, Borsche TS, Andersson G. Impact of low rotational inertia on power system stability and operation. IFAC Proc Vol 2014;47(3):7290–7.

[4] Saxena A, Shankar R. Improved load frequency control considering dynamic demand regulated power system integrating renewable sources and hybrid energy storage system. Sustain Energy Technol Assess 2022;52:102245.

[5] Ouyang J, Huangfu B, Diao Y, Yu J. An improved emergency frequency control for power system based on coordination of autonomous response and tripping of wind turbine. Sustainable Energy Technol Assess 2026;88:104943.

[6] Terzija V, Valverde G, Cai D, Regulski P, Madani V, Fitch J, et al. Wide-area monitoring, protection, and control of future electric power networks. Proc IEEE 2010;99(1):80–93.

[7] Sun M, Liu G, Popov M, Terzija V, Azizi S. Underfrequency load shedding using locally estimated RoCoF of the center of inertia. IEEE Trans Power Syst 2021;36(5):4212–22.

[8] Alhelou HH, Golshan MEH, Njenda TC, Hatziargyriou ND. An overview of UFLS in conventional, modern, and future smart power systems: challenges and opportunities. Electr Pow Syst Res 2020;179:106054.

[9] Pauschert L, Sioshansi R. Market designs for inertia remuneration in electricity systems. Curr Sustain Renew Energy Rep 2025;12(1):25.

[10] J. BILBAO, "Application of Numerical Methods in the Study of the Power Blackout of April 28, 2025, in Spain.".

[11] L. Rouco, F. Echavarren, and E. Lobato, "The Overvoltage-Driven Blackout of the Iberian Peninsula on 28th April 2025," *Sustainable Energy, Grids and Networks*, pp. 102125, 2026.

[12] MacIver C, Bell K, Nedd M. An analysis of the August 9th 2019 GB transmission system frequency incident. Electr Pow Syst Res 2021;199:107444.

[13] Homan S, Mac Dowell N, Brown S. Grid frequency volatility in future low inertia scenarios: challenges and mitigation options. Appl Energy 2021;290:116723.

[14] Banijamali SS, Amraee T. Semi-adaptive setting of under frequency load shedding relays considering credible generation outage scenarios. IEEE Trans Power Delivery 2018;34(3):1098–108.

[15] Dedović MM, Avdaković S, Musić M, Kuzle I. Enhancing power system stability with adaptive under frequency load shedding using synchrophasor measurements and empirical mode decomposition. Int J Electr Power Energy Syst 2024;160:110133.

[16] Rafinia A, Rezaei N, Moshtagh J. Optimal design of an adaptive under-frequency load shedding scheme in smart grids considering operational uncertainties. Int J Electr Power Energy Syst 2020;121:106137.

[17] Walger Q, Zuo Y, Derviškadić A, Frigo G, Paolone M. OPF-based under frequency load shedding predicting the dynamic frequency trajectory. Electr Pow Syst Res 2020;189:106748.

[18] Cai G, Zhou S, Liu C, Zhang Y, Guo S, Cao Z. Hierarchical under frequency load shedding scheme for inter-connected power systems. Prot Control Mod Power Syst 2023;8(1):34.

[19] Baškarad T, Holjevac N, Kuzle I, Ivanković I. Dynamically adaptive method for under frequency load shedding protection scheme reconfiguration. Electr Pow Syst Res 2022;207:107823.

[20] Cortés JS, Jegarluei MR, Aristidou P, Li K, Azizi S. Size/location estimation for loss of generation events in power systems with high penetration of renewables. Electr Pow Syst Res 2023;219:109242.

[21] Rudez U, Mihalic R. Monitoring the first frequency derivative to improve adaptive underfrequency load-shedding schemes. IEEE Trans Power Syst 2011;26(2):839–46.

[22] Sigrist L, Egido I, Rouco L. Principles of a centralized UFLS scheme for small isolated power systems. IEEE Trans Power Syst 2012;28(2):1779–86.

[23] Abdelwahid S, Babiker A, Eltom A, Kobet G. Hardware implementation of an automatic adaptive centralized underfrequency load shedding scheme. IEEE Trans Power Delivery 2014;29(6):2664–73.

[24] Tang J, Liu J, Ponci F, Monti A. Adaptive load shedding based on combined frequency and voltage stability assessment using synchrophasor measurements. IEEE Trans Power Syst 2013;28(2):2035–47.

[25] Jawad A, Banik S. A RoCoF-constrained underfrequency load shedding scheme with static voltage stability-based zoning approach. Sustainable Energy Grids Networks 2023;35:101080.

[26] Kabir MA, Chowdhury AH. A dynamic-adaptive load shedding methodology to improve frequency resilience of power systems. Int J Electr Power Energy Syst 2020;122:106169.

[27] Potel B, Cadoux F, de Alvaro Garcia L, Debusschere V. Clustering-based method for the feeder selection to improve the characteristics of load shedding. IET Smart Grid 2019;2(4):659–68.

[28] Badesa L, O'Malley C, Parajeles M, Strbac G. Chance-constrained allocation of UFLS candidate feeders under high penetration of distributed generation. Int J Electr Power Energy Syst 2023;147:108782.

[29] H. Jain, "Dynamic simulation of power systems using three phase integrated transmission and distribution system models: Case study comparisons with traditional analysis methods," 2017.

[30] Bustamante S, López GJ, Cardona HA. UFLS and smart load for frequency regulation in electrical power system: a review. IEEE Access 2023;11:110967–84.